Journal of Photochemistry and Photobiology A: Chemistry 277 (2014) 53–61

Contents lists available at ScienceDirect

Journal of Photochemistry and Photobiology A: Chemistry

journal homepage: www.elsevier.com/locate/jphotochem

The photochemistry of an aryl pentazole in liquid solutions: The anionic 4-oxidophenylpentazole (OPP)

Uzi Geiger [a], Yehuda Haas [a,*], Dan Grinstein [b]

[a] Institute of Chemistry, The Hebrew University of Jerusalem, Safra Campus, Jerusalem 91904, Israel
[b] IMOD, Israel

ARTICLE INFO

Article history:
Received 20 October 2013
Received in revised form
22 November 2013
Accepted 10 December 2013
Available online 17 December 2013

Keywords:
Aryl pentazoles
Cyclo-pentazolate anion
Photochemistry
Para oxidophenylazide
Para oxidophenylpentazole

ABSTRACT

This paper reports a study on the photolysis of an aryl pentazole in solution. 4-Oxidophenylpentazole (OPP) was irradiated in water and in acetonitrile at its first absorption band (320 and 370 nm, respectively) and at 193 nm. 4-Oxidophenylazide (OPA) was also investigated under similar conditions for comparison. NMR and UV–vis absorption spectroscopies of the products show that the major stable products of OPP photolysis in acetonitrile are OPA (which is also a thermal product), 4,4′-dihydroxyazobenzene, and 4-aminophenol while in water the main products are OPA and indophenol. The final product distribution obtained upon 193 nm irradiation is essentially the same as that found for the longer wavelength sources used. In these experiments some of the products are formed upon cleavage of the CN bond connecting the phenyl and the pentazole rings. These reactions are due to secondary collisional processes and not to a primary photochemical event. A mechanism accounting for the results is proposed.

1. Introduction

Aryl pentazoles were first synthesized by Lifschitz in 1915 [1] and later extensively studied by Huisgen and Ugi in the late 1950s and early 1960s [2–7]. Interest in aryl pentazoles has recently been revived due to the reports that the *cyclo*-pentazolate anion (cyclo-N_5^-) was formed in the gas phase from 4-hydroxyphenylpentazole (HOPP) [8] and 4-dimethylaminophenylpentazole [9]. The all-nitrogen *cyclo*-pentazolate anion was detected by mass spectrometry. Attempts to repeat this reaction thermally in the bulk have been unsuccessful [5,10], although ceric ammonium nitrate (CAN) oxidation of 4-methoxyphenyl pentazole did yield products believed to indicate the prior formation and degradation of cyclo-N_5^- [11]. This inference is in contrast with a previous paper [12] that concluded that no direct observation of the anion in solution was demonstrated. In any case, at the present time there is a consensus that cyclo-N_5^- has not been isolated by reactions of aryl azides in the bulk.

It has been suggested some time ago that cleavage of the C—N bond connecting the pentazole and the aromatic rings might be accomplished using photochemical methods [13]. However, to the best of our knowledge, no experimental photochemical study of aryl pentazoles has been reported to date. In this paper we report an initial photochemical study of aryl pentazoles, using 4-oxidophenylpentazole (OPP) as the reactant. Theoretical calculations indicate that the neutral N_5 ring radical spontaneously decomposes, whereas cyclo-N_5^- is calculated to be relatively stable [14–17]. The choice of an anionic aryl-pentazole precursor, rather than a neutral one was motivated by the notion that formation of cyclo-N_5^- would be in this case a homolytic bond cleavage whereas if a neutral precursor is chosen the cleavage is heterolytic and extra energy is needed to separate the nascent cation and anion. For this reason, and due to the high stability of OPP and HOPP relative to other aryl pentazoles, we have chosen OPP for this work.

OPP and the corresponding phenol (HOPP) have been studied by several groups [3,8,10]. Both species were found to be unstable at room temperature, releasing N_2 to form 4-oxidophenylazide (OPA) and 4-hydroxyphenylazide (HOPA), respectively. The activation energies measured for both processes are about 20 kcal/mol [10]. OPP and OPA were characterized by proton, ^{13}C, and ^{15}N NMR spectroscopies in solution [10].

Formation of an azide by dinitrogen extrusion is the energetically preferred thermal reaction, and is expected to be important also in photochemical reactions. It might be assumed that the azides are the primary products which subsequently lead to other products, by thermal or photochemical secondary reactions. Whereas the photochemistry and thermochemistry of many aryl azides were extensively investigated [18–22], the photochemistry of *para*-phenol azides and the corresponding anions is only poorly studied

---

* Corresponding author. Tel.: +972 26585067; fax: +972 25860622.
E-mail addresses: yehuda.haas@mail.huji.ac.il, yehuda@chem.ch.huji.ac.il (Y. Haas), Dan_grinstein@mod.gov.il (D. Grinstein).

1010-6030/$ – see front matter © 2014 Elsevier B.V. All rights reserved.
http://dx.doi.org/10.1016/j.jphotochem.2013.12.008

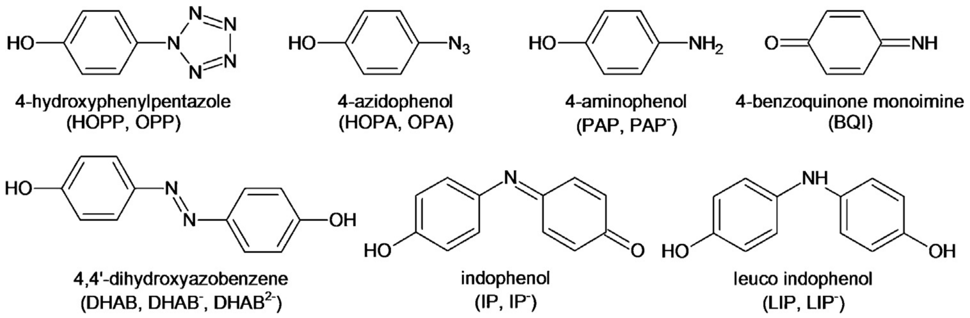

Chart 1. Main compounds discussed in this article with their abbreviations (in parentheses) as neutral, mono anionic and di-anionic forms when applicable. BQI in this paper is the short-hand description of 4-benzoquinone monoimine (*para* BQI). The *ortho* form (2-benzoquinone monoimine) is marked as such where appropriate.

[23,24]. We have therefore examined also the photochemistry of OPA, and compared it with that of the OPP. The names and structures of the compounds discussed in this paper are listed in Chart 1.

2. Experimental

2.1. Materials and equipment

P-aminophenol HCl (Fluka, purum, ≥99.0%), sodium nitrite (Aldrich, 97.0%), sodium azide (Aldrich, purum, ≥99.0%), methanol (BioLab, HPLC supra gradient), deuterium oxide (99.9 atom% D, Aldrich), acetonitrile-D_3 (D, 99.8%, Cambridge Isotope Laboratories, inc.), hydrochloric acid (Sigma–Aldrich, 37% fuming), and nitrogen-15 labeled sodium nitrite (98% + ^{15}N, Cambridge Isotope Laboratories, Inc.) were used as received. Tetramethyl ammonium hydroxide (Sigma–Aldrich, 25 wt.% in methanol, TMAOH) was used as received or diluted 10 times in dry MeCN or MeOH. Acetonitrile (Fluka, for UV-spectroscopy, ≥99.8%) was dried over 4 A molecular sieves, passed over a short column of molecular sieves and filtered just prior to use. The water used was ultra-purified with a Branstead Nanopure type I water system (Thermo Scientific).

A q-pod 2e temperature controlled cuvette holder system equipped with a magnetic stirrer was used for irradiation (Quantum North West). An USB-4000 fiber optic spectrometer was used with a DH-2000-BAL or DT-mini-2-GS light source for UV–vis absorption measurements, all from Ocean Optics. Two concentration ranges were used, as the NMR measurements required much higher concentration than practical for UV absorption spectrometry. The concentration required for NMR ($\sim 10^{-2}$ M) was too high for UV experiments, for which a $\sim 10^{-4}$ M concentration was suitable to avoid saturation. The spectrometer and light source were either attached to the q-pod perpendicular to the irradiation direction for the low concentration experiments or to an uncooled cuvette holder nearby for the high concentration experiments (measurements were taken as quickly as possible). A Bruker Avance II 500 MHz NMR spectrometer was used for all NMR measurements. The photolysis light sources were either a pulsed ArF excimer laser with variable firing rate (Neweks Ltd., PSX-100) or a 150 W xenon lamp fitted with a water filter and the appropriate low-pass and high-pass filters for the experiment (Hamamatzu E7536 with L2175).

2.2. Synthesis of OPP and OPA

HOPP was synthesized by a method similar to that used by Ugi and Huisgen [2] and previously by us [25]. In a typical synthesis a 100 ml glass flask (the reaction vessel) was immersed in acetone in a jacketed reactor, through which ethanol was circulated at −7.5 °C (no freezing occurred in the reaction vessel under these conditions). 6 ml of water, 1 ml of HCl (12 mequiv.) and 1.302 g (8.9 mmol) of p-aminophenol HCl were introduced to the reaction vessel under continuous stirring. Upon drop-wise addition of 0.703 g (10.5 mmol) of $NaNO_2$ dissolved in 4 ml water, the solution, stirred for 1 h, became dark blue due to the formation of the diazonium salt. 20 ml of methanol were added and the vessel was allowed to stabilize at −15 °C for 1.5 h. 0.813 g (12.5 mmol) of sodium azide dissolved in 8 ml water were added slowly. During the addition of the azide strong bubbling of the solution occurred due to generation of gaseous nitrogen and a white precipitate was formed. After allowing the solution to react for 1 h, the precipitate was filtered through a cooled, jacketed filter funnel and washed with ca. 150 ml freezer-cold 1:1 methanol:water solution to yield the crude product. The crude product was re-dissolved in 13 ml cold methanol and filtered into a dry-ice cooled filter bottle, into which 10 ml of pure water were added and the precipitated material was again filtered through a cold filter and washed with the methanol:water mixture. The product HOPP was transferred to a weighted vial and dried under vacuum at ca. −30 °C. Yield: 16% (0.233 g, 1.43 mmol).

HOPA was prepared from HOPP by allowing the material to warm to 25 °C.

OPP was freshly prepared for each experiment by adding excess base (usually TMAOH) to a HOPP solution. OPA was likewise prepared from HOPA, or by warming OPP to 25 °C.

2.3. Procedure of photochemical experiments

OPP and OPA were irradiated in water at +5 °C or MeCN at −27.5 °C using either a pulsed ArF excimer laser at 193 nm or the xenon lamp equipped with the appropriate filters. Low concentration experiments were performed as follows: 2 ml of the appropriate solvent were loaded into a 10 mm × 10 mm quartz cuvette equipped with a magnetic stirrer; the cuvette was placed in the q-pod holder and allowed to equilibrate to the set temperature. A solution of ca. 1 mg HOPP in 1 ml MeOH (for water) or MeCN was prepared in a 5 ml vial and kept in dry ice. From this mother solution about 5 μl were added to the cuvette and, if OPA was needed, the solution was heated to 25 °C for 30 min quantitatively yielding HOPA. Ca. 10 μl of 10× diluted TMAOH was added to convert HOPP or HOPA to OPP or OPA, respectively. The irradiation of the low concentration solution lasted no more than 5 min and was analyzed by UV–vis spectroscopy only.

High concentration experiments were performed as follows: 1.5 ml of the solvent, usually deuterated, were loaded into a 10 mm × 10 mm cuvette with a magnetic stirrer. The cuvette was placed into the q-pod holder and allowed to equilibrate to the set temperature. Roughly 5 mg of HOPP were weighed and added to the cuvette. If OPA was needed in MeCN the system was heated to 25 °C for 30 min to quantitatively yield HOPA; in water the base

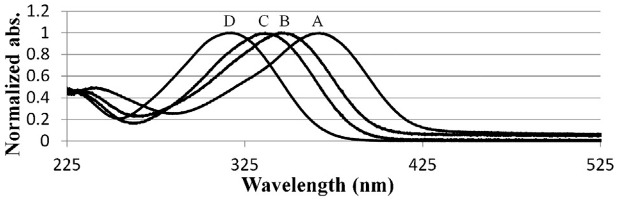

Fig. 1. Normalized UV–vis absorption spectra of solutions of OPP in: dry MeCN (A, λ_{max} = 368 nm); 1% water in MeCN (B, λ_{max} = 345 nm); 5% water in MeCN (C, λ_{max} = 336 nm); and water (D, λ_{max} = 317 nm).

was added first to allow good solubility. 15 μl of TMAOH was used to convert the HOPP or HOPA to OPP or OPA, respectively. The irradiation of the high concentration solution lasted up to 4 h and was analyzed by NMR spectroscopy, or, after appropriate dilution, by UV–vis spectrometry. 1D proton and nitrogen and 2D COSY, HSQC and HMBC spectra were used to identify the constituents of the product mixture.

For validating the identification of the products it was often beneficial to prepare the acid forms of the ions, as NMR data are more abundant for the neutral acid. 5 μl of glacial acetic acid was added directly to the NMR tube containing ca. 1 ml solution.

3. Results

3.1. OPP spectra in water-acetonitrile mixtures

The first absorption band of OPP is blue shifted upon changing the solvent from MeCN to water by a relatively large shift (0.542 eV), from 368 to 317 nm (Fig. 1). This large difference may be due either to polarity change, in which case a low water impurity in MeCN would have a negligible effect, or to hydrogen bonding, which might strongly affect the shift even at low water concentrations. To clarify this point UV–vis absorption spectra of OPP in MeCN:water solutions of different ratios were measured (Fig. 1). In addition, the absorption spectrum of OPP in MeOH (capable of making hydrogen bonds, dielectric constant similar to MeCN) was taken for comparison and is shown in the Supplementary Data (SD1).

A 1% water impurity in MeCN accounts for 40% of the shift and 5% account for 60% of the shift. These data, together with the large MeOH shift (λ_{max} = 321 nm) compared to MeCN, indicate the importance of hydrogen bonding.

3.2. Irradiation in MeCN

The UV–vis absorption spectra measured after Xe lamp irradiation of OPP and OPA at low (Ca. 10^{-4} M) and high (Ca. 10^{-2} M) concentrations, together with the absorption spectrum of OPP itself and OPA, are shown in Fig. 2; changing the excitation source to 193 nm led to practically identical product spectra in the high concentration solution, but different spectra are observed in the low concentration solution; in this case broad absorption bands characteristic of tar particles, similar to other azides [18,20] were observed (see SD2, SD3).

The most prominent, narrow absorption bands appearing immediately upon irradiation of low OPP concentration at 242 and 251 nm (shown in SD3) are attributed to the anion of BQI. Their intensity diminishes in less than a minute and two broader bands centered at 500 and 615 nm are observed (Fig. 2); they also appear upon OPA irradiation, (Fig. 3, below). These bands are assigned to polymers such as polyacetonitrile and poly aminophenol.

At higher concentrations (Fig. 2C.) a major new absorption peak appears at 475 nm as well as another single peak at about 250 nm. These bands are tentatively assigned to DHAB⁻ and PAP⁻, respectively.

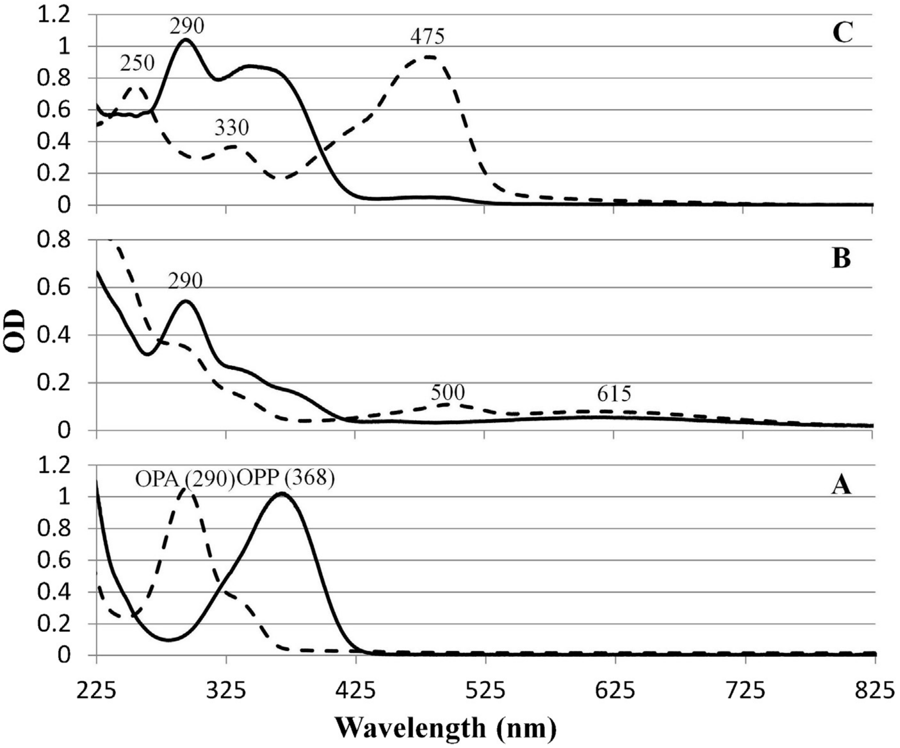

Fig. 2. UV–vis absorption spectra in MeCN at −27.5 °C of: (A) OPP (40 μM, full line) and OPA (40 μM, dashed line); (B) a 45.5 μM OPP solution irradiated at 350–390 nm for 60 s (full line) and a 50 μM OPA solution irradiated at 280–390 nm for 10 s (dashed line); (C) a 28,000 μM OPP solution irradiated at 350–390 nm for 150 min (full line) and a 41,000 μM OPA solution irradiated at 280–390 nm for 90 min (dashed line). C was measured following 50 times dilution for the OPP solution and 100 times for the OPA solution in a 2 mm cuvette for a total of 250× and 500× optical dilution for OPP and OPA, respectively.

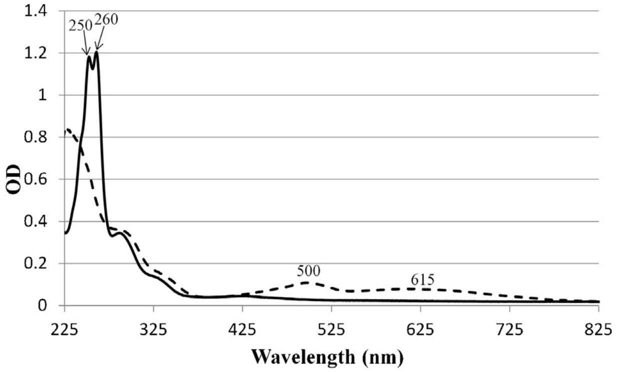

Fig. 3. UV–vis absorption spectra at −27.5 °C of OPA solutions (48 μM) after 280–390 nm irradiation for 10 s in wet (0.25% water) MeCN (full line) and in dry MeCN (dashed line). The spectrum of the dry solution was recorded 1 min after irradiation, the spectrum of the wet solution 10 min after irradiation and is identical to the one taken immediately after irradiation.

Water appears to strongly affect the outcome of the irradiation, in both OPP and OPA as can be seen from Fig. 3: even a small amount of water changes the absorption of the products to 250 and 260 nm. These absorption bands are due to species that are more stable than those obtained in dry solutions (absorption peaks at 242 and 251 nm) and are compatible with the formation of BQI in MeCN, possibly hydrogen-bonded to water. In the high concentration experiments no special measures for solvent dehydration were needed and the use of commercial CD_3CN (not anhydrous) resulted in the same product absorption spectra as upon using carefully dried MeCN.

The tentative assignments of the products at low and high OPP concentrations suggested by UV–vis spectra were confirmed and improved by NMR measurements carried out using high concentrations of OPP. Fig. 4 shows representative proton NMR spectra of irradiated solutions of OPP and OPA in MeCN; the same spectra are found following irradiation of OPP or OPA at 193 nm. It is noted that in general the product distribution of the major non-OPA products of OPP irradiation (Table 1) are similar in MeCN to those recorded upon OPA irradiation (except for the long wavelength irradiation of OPP). All other NMR spectra, including the proton NMR spectrum of an OPA solution after irradiation and acidification with acetic acid, are shown in the Supplementary Data (SD4).

3.3. Photochemistry in water

Being anions, OPP and OPA readily dissolve in water, in contrast with other aryl pentazoles and organic azides. Fig. 5 shows the UV–vis spectra of OPP and OPA solutions in water at 5 °C and those obtained after irradiating OPP at 5 °C at high and low concentrations. The most prominent new absorption bands in the low concentration samples are at 255 and 262 nm, slightly shifted from the product found for low concentration in wet MeCN (Fig. 2) and are assigned BQI in water. In the high concentration case the first main band appears at 632 nm (IP^-) and another one appears after further irradiation at 450 (probably LIP^-) nm, with no qualitative difference between OPP and OPA or between the two excitation sources (other spectra are shown in the Supplementary Data (SD5)).

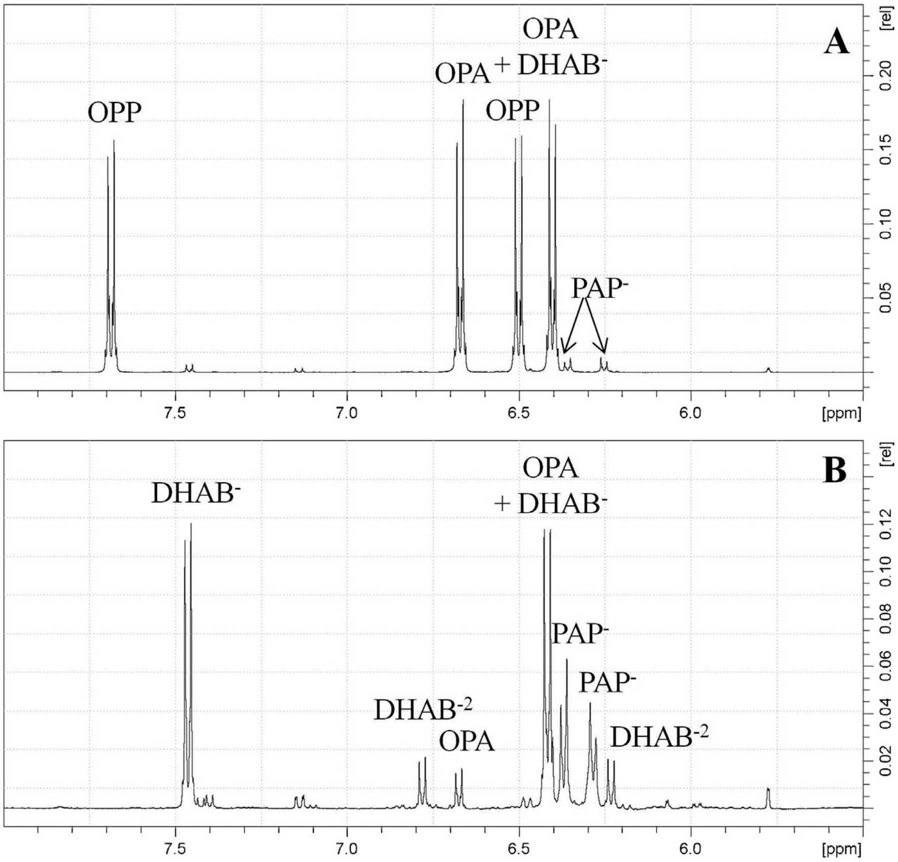

Fig. 4. Proton NMR spectra and major peak assignments of: (A) OPP irradiated at 350–390 nm for 150 min; (B) OPA irradiated at 280–390 nm for 90 min. Both irradiations were carried out in CD_3CN at −27.5 °C and both spectra were taken at −35 °C. The full assignments are discussed in a subsequent Section 3.4.

Table 1
The photochemical product distribution obtained upon irradiation of OPP and OPA solutions in MeCN using different light sources. The main product from OPP irradiation is always OPA, (not included in the table). The unknown product shows splitting characteristic of a 1,2,4 substituted aromatic ring (AX, AXY, and AY splitting for the 7.14, 6.47, and 5.77 peaks, respectively). Percentages derived from proton NMR measurements.

Experimental conditions	Product (aromatic proton shift)		
	DHAB$^-$ (7.46, 6.42)	PAP$^-$ (6.36, 6.27)	Unknown (7.14, 6.47, 5.77)
OPP 193 nm irradiation	50%	36%	5.5%
OPA 193 nm irradiation	47%	34%	4.2%
OPP 350–390 nm irradiation	28%	59%	13%
OPA 250–390 nm irradiation	52%	32%	3.2%

Abbreviations according to Chart 1

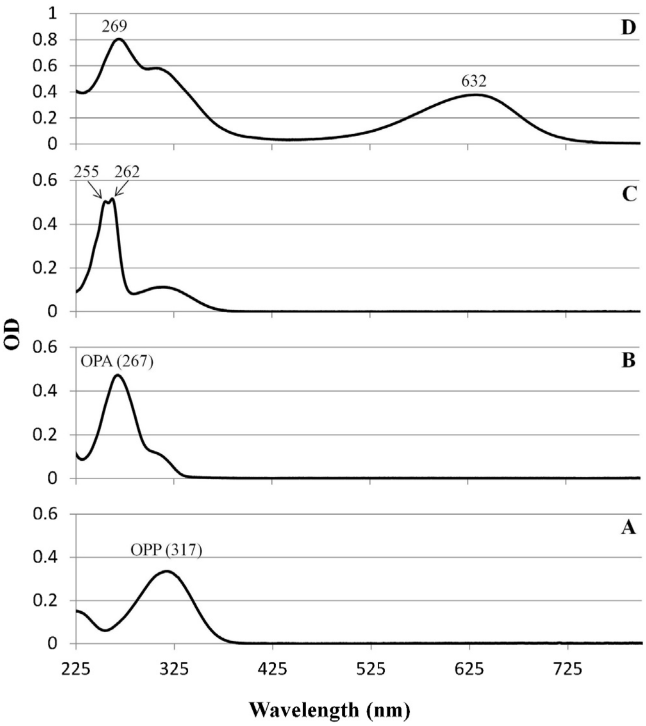

Fig. 5. UV–vis absorption spectra in water at 5 °C of: (A) OPP (24 μM), (B) OPA (24 μM), (C) a 24 μM OPP solution irradiated by a Xe lamp (270–380 nm filter) for 90 s, and (D) a 23,000 μM OPP solution irradiated by a Xe lamp (325–390 nm filter) for 4 h and 20 min. D was measured following 50 times dilution in a 2 mm cuvette for a total of 250× optical dilution.

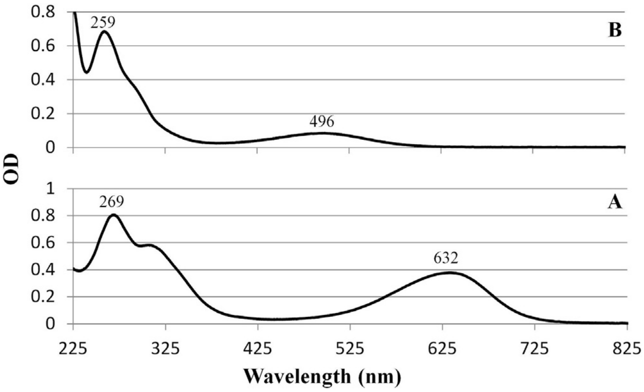

Fig. 6. UV–vis absorption spectra of an OPP solution (23 mM) in water at 5 °C after 260 min irradiation at 325–390 nm: (A) as is and (B) acidified with acetic acid. Both spectra diluted 50× in water and using a 2 mm cuvette for a total 250× optical dilution.

Table 2
Major products obtained upon OPA irradiation in MeCN and in water at different concentrations. Products of OPP irradiation are identical apart from OPA being the dominant product.

Solvent	Low concentration	High concentration
MeCN	Polyacetonitrile Polyaminophenol PAP$^-$	DHAB$^-$ PAP$^-$
Water	BQI	IP$^-$ LIP$^-$

After addition of excess acetic acid the UV–vis changes to the spectrum shown in Fig. 6, with the 632 nm absorption band shifted to 496 nm, agreeing well with the protonation of IP$^-$ to IP.

A representative H NMR spectrum of an OPP solution irradiated in D_2O is shown in Fig. 7. Two main products appear in addition to OPA after the irradiation: one with broad peaks and the other with sharp ones, both are in the aromatic region. Their proposed assignments are shown in the figure and are compared with literature in Section 3.4.

Fig. 8 presents NMR of OPP, labeled at the 2/5 positions by using ^{15}N isotopically enriched sodium nitrite in the synthesis, after Xe lamp irradiation in water. The signals shown are those of OPP, OPA, N_2 and the centrally labeled azide ion only. The same signals, apart from the azide ions, were also detected after OPP and OPA irradiation in MeCN and in a solution of OPP in MeCN allowed to react thermally for a while (shown in SD6).

Table 2 summarizes the key results and compares the major products of OPA photolysis in MeCN with those found in water, the assignments are fully discussed in the next subsection. OPP irradiation leads to the same products in addition to production of OPA (the dominant product). As seen in the table different end products are found for the two solvents.

3.4. Product identification

The products were identified mainly on the basis of NMR data, and are also compatible with the UV–vis absorption spectra. Table 3 summarizes the data collected for the identified products and literature references (if available). The NMR data consisted of both proton and carbon data via the HSQC and HMBC methods. Identification was helped by acidification of the solution as literature data on the acid form is more extensive than on most mono and di-anionic molecules of interest. The identification of the anionic forms matching the neutral ones, especially for molecules with more than one such form, is based on integration of proton NMR signals.

The identification of LIP is based only on H NMR data and comparison to calculated references and is therefore less reliable.

Other products were obtained in low yields, not sufficient for ^{13}C NMR analysis (analyzed by proton NMR integration). The

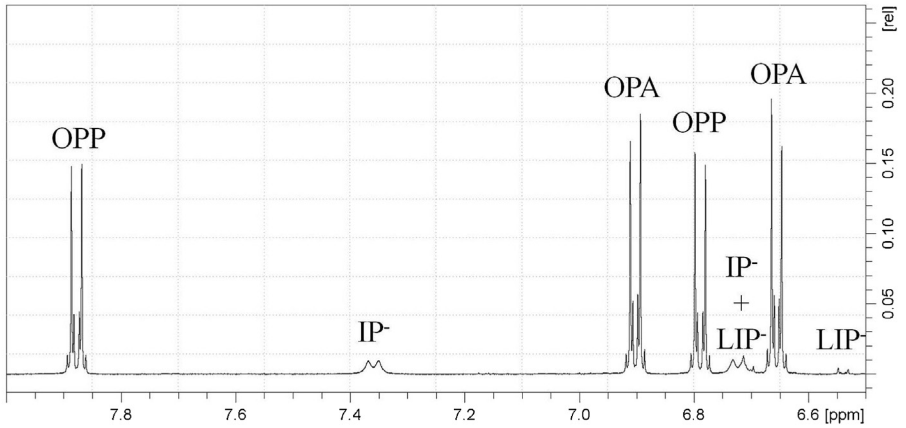

Fig. 7. Proton NMR spectrum of a 19 mM OPP solution in D_2O at 5 °C after a 325–390 nm irradiation for 100 min.

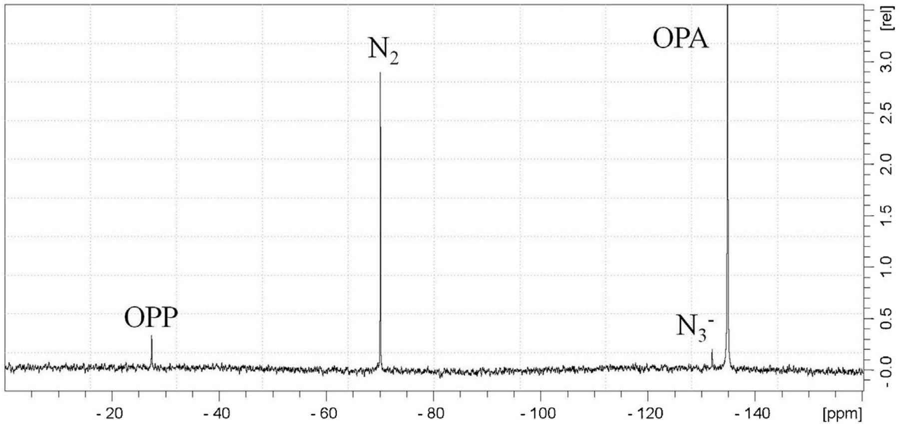

Fig. 8. ^{15}N NMR spectrum of a 36.5 mM OPP solution in water at 5 °C after 4 h irradiation at 305–390 nm.

Table 3
Identified and suspected products with their experimental data and literature references. Each reference is for both NMR and UV–vis data, where applicable.

Compound	Experimental data	Literature data	Notes and references
DHAB (CD_3CN)	^1H NMR: 7.72, 6.98 ^{13}C NMR: 161.0, 145.1, 124.1, 115.9	^1H NMR: 7.71, 6.94 ^{13}C NMR: 160.8, 146.1, 125.0, 116.6	In DMSO-d_6 [26]
DHAB$^-$ (CD_3CN)	^1H NMR: 7.46, 6.42 ^{13}C NMR: 171.9, 140.6, 123.6, 118.9 UV–vis: 475 nm	UV–vis: 465–470 nm	In water [27]
DHAB^{-2} (CD_3CN)	^1H NMR: 6.78, 6.24 ^{13}C NMR: 169.6, 140.3		
PAP (CD_3CN)	^1H NMR: 6.58, 6.50 ^{13}C NMR: 149.2, 139.9, 115.8, 115.3	^1H NMR: 6.485, 6.426 ^{13}C NMR: 148.25, 140.46, 115.51, 115.26	In DMSO-d_6 [28]
PAP$^-$ (CD3CN)	^1H NMR: 6.36, 6.27 ^{13}C NMR: 160.4, 133.5, 118.8, 116.8 UV–vis: 250, 330 nm	UV–vis: 256, 320 nm	From an authentic material sample
BQI (water)	UV–vis: 255, 262 nm	UV–vis: 255, 263 nm	In water[29]
IP (water)	^1H NMR: 7.22, 6.86 UV–vis: 496 nm	^1H NMR: 7.32, 6.96 UV–vis: 496 nm	In water [30]
IP$^-$ (water)	^1H NMR: 7.34, 6.72 UV–vis: 632 nm	^1H NMR: 7.18, 6.8 UV–vis: 637 nm	In water [30]
LIP (water)	^1H NMR: 7.28, 7.00 (obtained after acidification, poor quality due to aggregation)	^1H NMR: 7.1, 6.89 (Predicted spectrum, as experimental data not available)	[31]
LIP$^-$ (water)	^1H NMR: 6.70, 6.54 ^{13}C NMR: 159.1, 133.3, 118.6, 118.6	Not available	

UV–vis data for these compounds are also largely unknown due, probably to overlap with the absorption of other substances in the mixture and/or poor signal to noise ratio. The data on these compounds are available in the Supplementary Data (SD7 and SD8).

4. Discussion

4.1. Main products

The photochemical reactions of many aryl azides are known to proceed via an aryl nitrene intermediate [20–22]. Our data show

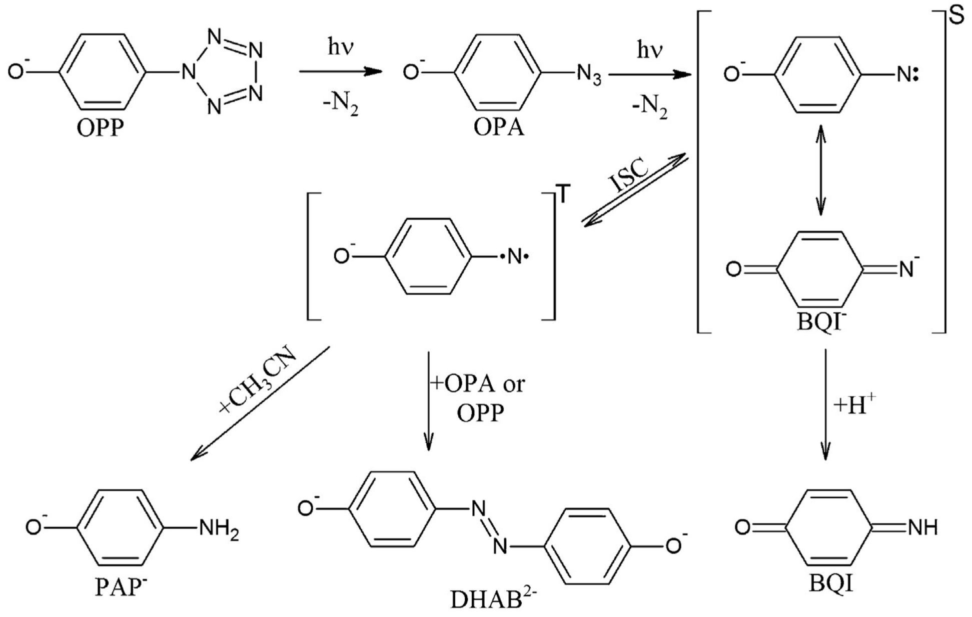

Scheme 1. Main routes proposed for the photochemistry of OPP in the studied media.

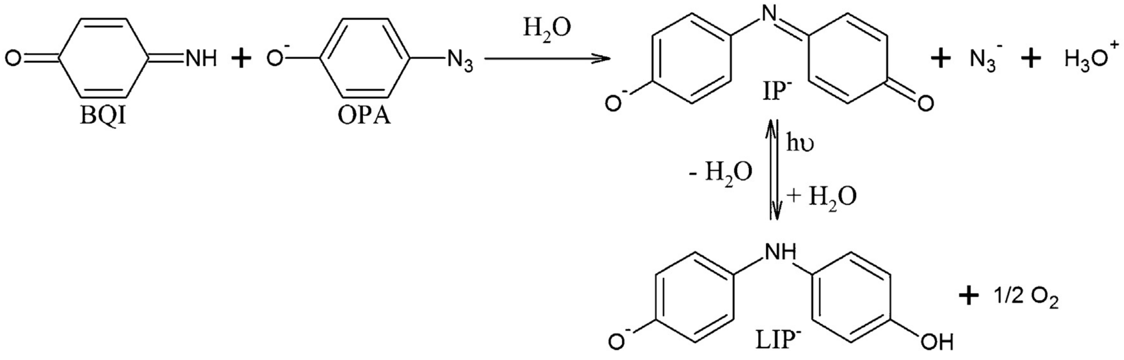

Scheme 2. An outline of the reaction of BQI with OPA in water, forming indophenolate and the azide ion. The possible photoreaction of IP^- with water to give LIP^- is also depicted.

that irradiation of OPP in MeCN produces mainly OPA, and by analogy with the rich literature on aryl azide photochemistry [20], irradiation of OPA leads to the final products by reactions of the nitrene intermediate (Scheme 1). There is no evidence that another mechanism is operative in the case of high energy irradiation of OPP in MeCN or water (at 193 nm). It is noted that in this case a good separation between the excitation of OPP and OPA could not be achieved.

The end products of OPP and OPA irradiation in MeCN are assumed to be derived from triplet nitrene by analogy with other aryl azides [20]; the currently accepted literature mechanisms for their production are included in Scheme 1. The low concentration experiments in dry MeCN show an overlap of two main absorptions: one is identified as the polymer of PAP which has an absorption band at 500 nm [32] and the other, whose absorption peaks at 615 nm, may be due to poly-acetonitrile, though regrettably literature references for the latter are not yet available. OPA, PAP and DHAB are the main stable products of OPP irradiation at concentrations high enough to use NMR spectroscopy. Another, as yet unidentified, product in MeCN has the characteristic H NMR peak splitting of a 1,2,4 substituted aromatic ring. This product appears to undergo further photoreaction when more energetic photons are used, but upon irradiation at 350–390 nm it remains as one of the stable products (OPP irradiation). It should be noted that whereas the *relative* amounts of the end product change for different excitation sources, no new products are found in any of these cases, indicating a quantitative rather than a qualitative difference.

In water, the main products observed are not known to be derived from a nitrene, and so is para-BQI (4-BQI) produced in wet MeCN and in water under low concentration conditions. A related compound (ortho-BQI, 2-BQI) was found upon irradiation of 2-hydroxyphenylazide in various solvents, mostly in protic solvents and specifically in water [23]. The unstable anion of BQI may be viewed as a resonance form of singlet nitrene, which may be further stabilized by addition of a proton to form neutral BQI. On the other hand BQI is known to produce leuco indophenols with phenols (when a para hydrogen is present) by electrophilic aromatic substitution and these are easily oxidized by atmospheric oxygen or by another BQI molecule to indophenols [30,33]. If BQI (an electrophile) attacks OPA (a nucleophile) releasing an azide anion rather than a proton as is the case for phenols, indophenol should be directly formed, as indeed is the case at higher concentrations of OPP or OPA (Scheme 2).

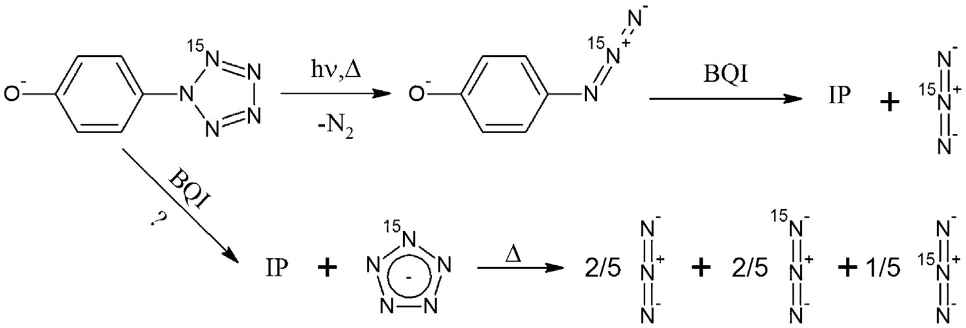

Scheme 3. Two possible reaction routes of nitrogen-15 labeled OPP at the 2/5 position with BQI: thermal or photochemical nitrogen extrusion to form OPA, which proceeds to react with BQI to form IP and centrally labeled azide ion, or a direct reaction of OPP with BQI to form IP and cyclo-N_5^-; the latter might decompose thermally to centrally, terminally and non labeled azide ions.

4.2. C—N bond cleavage

The reaction between BQI and OPP or OPA to produce indophenols (Scheme 2) involves the cleavage of the C—N bond. OPP labeled with ^{15}N at the 2/5 positions of the pentazole ring was used to investigate this reaction (Fig. 8). While labeled OPA derived from the labeled OPP produced the centrally labeled azide ion as expected (Scheme 3), OPP also produced only this extra signal, indicating that the only significant reaction is of BQI and thermally or photochemically produced OPA. If the C—N bond of OPP would have been cleaved and cyclo-N_5^- produced, two more signals should have been observed – that of cyclo-N_5^- itself and that of its other thermal dissociation product, the terminally labeled azide ion.

It is of interest to compare our results with previous work that reported formation of cyclo-N_5^- from HOPP. The scission of the CN bond was reported by Vij et al. [8] in the gas phase using mass spectrometry detection. The reaction probably proceeds by first forming OPP (which is in equilibrium with HOPP, and whose concentration can be increased using pyridine) followed by colliding the anion with high energy argon or nitrogen. The result is somewhat surprising, as extrusion of nitrogen from OPP is energetically preferred. However, intact cyclo-N_5^- was only observed using high collision energies (75 eV), whereas at low collision energies the azide was formed. In solution, collision energies are limited by the solvent, and thus our results are compatible with those of Ref. [8].

4.3. Minor products

As can be seen in the NMR spectra in the SD files, a number of minor products are also produced upon irradiating OPP and OPA. In total, 9 products were identified in MeCN, only 3 of these constituted more than 5% of the total aromatic protons (PAP^-, $DHAB^-$ and $DHAB^{-2}$). In water, 7 products were identified, two of which were detected in more than 5% of total aromatic protons – indophenol and the assumed leuco-indophenol, which in this case may be a product of photo-reduction of the former (and is known to oxidize to indophenol when oxygen or BQI are present). It is yet to be determined if the minor products (those constituting less than 5% of total aromatic protons) are produced via another photochemical path, another nitrene reaction or via the irradiation and photoreactions of the primary products.

5. Conclusions

This paper reports the experimental photochemistry of an aryl pentazole in liquid solutions. The molecule chosen for this work, para oxidophenylpentazole (OPP) was photolyzed in water and MeCN. The main primary product is oxidophenylazide (OPA), which is also the main end product when the excitation wavelength used is not absorbed by it. Otherwise, several more products are found, presumably due to reactions of a nitrene formed by extrusion of another N_2 molecule. In general, the products of OPP and OPA photolysis were the same, as shown by independently studying OPA photolysis. Under the experimental conditions employed here no direct photochemical C—N bond cleavage was observed. None the less, C—N bond cleavage occurred, presumably by reaction with benzoquinone imine (BQI). This is, to the best of our knowledge, the first observation of this reaction. Likewise, the photochemical production of BQI from OPA was realized for the first time.

In MeCN the photochemistry of OPA is similar to that of other aryl azides leading mainly to the formation of para aminophenol (PAP) and 4,4′-dihydroxyazobenzene (DHAB). In water the photochemistry leads to the formation of BQI which reacts with another OPA molecule to form indophenol (IP).

Appendix A. Supplementary data

Supplementary data associated with this article can be found, in the online version, at http://dx.doi.org/10.1016/j.jphotochem.2013.12.008.

References

[1] J. Lifschitz, Synthese der pentazol-verbindungen. I, Ber. Dtsch. Chem. Ges. 48 (1915) 410–420.
[2] R. Huisgen, I. Ugi, Pentazole I, Die lösung eines klassischen problems der organischen stickstoffchemie, Chem. Ber. 90 (1957) 2914–2927.
[3] I. Ugi, R. Huisgen, Pentazole II, Die zerfallsgeschwindigkeit der aryl-pentazole, Chem. Ber. 91 (1958) 531–537.
[4] I. Ugi, H. Perlinger, L. Behringer, Pentazole III, Kristallisierte aryl-pentazole, Chem. Ber. 91 (1958) 2324–2329.
[5] I. Ugi, H. Perlinger, L. Behringer, Pentazole IV, Der konstitutionsbeweis für kristallisiertes [p-Äthoxy-phenyl]-pentazol, Chem. Ber. 92 (1959) 1864–1866.
[6] I. Ugi, Pentazole V, Zum mechanismus der bildung und des zerfalls von phenylpentazol, Tetrahedron 19 (1963) 1801–1803.
[7] I. Ugi, Pentazoles, Adv. Heterocycl. Chem. 3 (1964) 373–383.
[8] A. Vij, J.G. Pavlovich, W.W. Wilson, V. Vij, K.O. Christe, Experimental detection of the pentaazacyclopentadienide (pentazolate) anion, cyclo-N_5^-, Angew. Chem. Int. Ed. Engl. 41 (2002) 3051–3054.
[9] H. Östmark, S. Wallin, T. Brinck, P. Carlqvist, R. Claridge, E. Hedlund, L. Yudina, Detection of pentazolate anion (cyclo-N_5^-) from laser ionization and decomposition of solid p-dimethylaminophenylpentazole, Chem. Phys. Lett. 379 (2003) 539–546.
[10] V. Benin, P. Kaszynski, J.G. Radziszewski, Arylpentazoles revisited: experimental and theoretical studies of 4-hydroxyphenylpentazole and 4-oxophenylpentazole anion, J. Org. Chem. 67 (2002) 1354–1358.
[11] R.N. Butler, J.M. Hanniffy, J.C. Stephens, L.A. Burke, A ceric ammonium nitrate N-dearylation of N-p-anisylazoles applied to pyrazole, triazole, tetrazole, and pentazole rings: release of parent azoles. Generation of unstable pentazole, HN(5)/N(5)(−), in solution, J. Org. Chem. 73 (2008) 1354–1364.
[12] T. Schroer, R. Haiges, S. Schneider, K.O. Christe, The race for the first generation of the pentazolate anion in solution is far from over, Chem. Commun. (2005) 1607–1609.
[13] L. Belau, Y. Haas, S. Zilberg, Formation of the cyclo-pentazolate N_5-anion by high-energy dissociation of phenylpentazole anions, J. Phys. Chem. A 108 (2004) 11715–11720.

[14] G. da Silva, E.E. Moore, J.W. Bozzelli, Quantum chemical study of the structure and thermochemistry of the five-membered nitrogen-containing heterocycles and their anions and radicals, J. Phys. Chem. A 110 (2006) 13979–13988.
[15] M. Rahm, T. Brinck, Kinetic stability and propellant performance of green energetic materials, Chem. Eur. J. 16 (2010) 6590–6600.
[16] M.T. Nguyen, M. Sana, G. Leroy, J. Elguero, Theoretical study on the structure and reactivity of pentazole anions, Can. J. Chem. 61 (1983) 1435–1439.
[17] M.T. Nguyen, Polynitrogen compounds: 1. Structure and stability of N_4 and N_5 systems, Coord. Chem. Rev. 244 (2003) 93–113.
[18] B. Iddon, O. Meth-Cohn, E.F.V. Scriven, H. Suschitzky, P.T. Gallagher, Developments in arylnitrene chemistry: syntheses and mechanisms, Angew. Chem. Int. Ed. Engl. 18 (1979) 900–917.
[19] E. Leyva, M.S. Platz, G. Persy, J. Wirz, Photochemistry of phenyl azide: the role of singlet and triplet phenylnitrene as transient intermediates, J. Am. Chem. Soc. 108 (1986) 3783–3790.
[20] N.P. Gritsan, M.S. Platz, Kinetics, spectroscopy and computational chemistry of arylnitrenes, Chem. Rev. 106 (2006) 3844–3867.
[21] G.B. Schuster, M.S. Platz, Photochemistry of phenyl azide, in: D.H. Volman, G.S. Hammond, D.C. Neckers (Eds.), Adv. Photochem., vol. 17, John Wiley & Sons, Inc., NY, 2007, pp. 69–143.
[22] G. Burdzinski, J.C. Hackett, J. Wang, T.L. Gustafson, C.M. Hadad, M.S. Platz, Early events in the photochemistry of aryl azides from femtosecond UV/vis spectroscopy and quantum chemical calculations, J. Am. Chem. Soc. 128 (2006) 13402–13411.
[23] L.N. Karyakina, A.V. Oleinik, Photolysis of ortho-azidophenol in various solvents, High Energy Chem. 41 (2007) 109–113.
[24] N.J. Rau, E.A. Welles, P.G. Wenthold P, Anionic substituent control of the electronic structure of aromatic nitrenes, J. Am. Chem. Soc. 135 (2013) 683–690.
[25] U. Geiger, A. Elyashiv, R. Fraenkel, S. Zilberg, Y. Haas, The Raman spectrum of dimethylaminophenyl pentazole (DMAPP), Chem. Phys. Lett. 556 (2013) 127–131.
[26] I. Yildiz, S. Ray, T. Benelli, F.M. Raymo, Dithiolane ligands for semiconductor quantum dots, J. Mater. Chem. 18 (2008) 3940–3947.
[27] N.J. Dunn, W.H. Humphries, A.R. Offenbacher, T.L. King, J.A. Gray, pH-dependent cis → trans isomerization rates for azobenzene dyes in aqueous solution, J. Phys. Chem. A 113 (2009) 13144–13151.
[28] SDBSWeb: http://sdbs.riodb.aist.go.jp (National Institute of Advanced Industrial Science and Technology, 08.09.13).
[29] J.F. Corbett, Benzoquinone imines. Part II. Hydrolysis of p-benzoquinone monoimine and p-benzoquinone di-imine, J. Chem. Soc. B. (1969) 213–216.
[30] J.F. Corbett, Benzoquinone imines. Part VIII. Mechanism and kinetics of the reaction of p-benzoquinone monoimines with monohydric phenols, J. Chem. Soc. B. (1970) 1502–1509.
[31] ACD Predicted NMR data calculated using Advanced Chemistry Development, Inc. (ACD/Labs) Software V11.01 (© 1994–2013 ACD/Labs).
[32] C. Chen, C. Sun, Y. Gao, Electrosynthesis of a net-like microstructured poly(p-aminophenol) film possessing electrochemical properties in a wide pH range, J. Macromol. Sci. Pure Appl. Chem. 45 (2008) 972–979.
[33] J.H. Baxendale, S. Lewin, The aerobic oxidation of leuco phenol indophenols, Trans. Faraday Soc. 42 (1946) 126–133.